



## Data Storage Report

RODBreak – Wave run-up, overtopping and damage in rubble-mound breakwaters under oblique extreme conditions due to climate change scenarios



## Project Information

<b>Acronym</b>	H+_LUH_03_Basin_Rodbreak
<b>Title</b>	RODBreak - Wave run-up, overtopping and damage in rubble-mound breakwaters under oblique extreme wave conditions due to climate change scenarios
<b>Location(s)</b>	FZK – Wave and current basin
<b>Start date</b>	2017-10-09
<b>End date</b>	2017-11-17

## Project Personnel

<b>Name</b>	<b>Institution</b>	<b>Email</b>
João Alfredo Santos	ISEL	jasantos@dec.isel.ipl.pt
Francisco Pedro	ISEL	A32643@alunos.isel.pt
Mário Coimbra	ISEL	A39777@alunos.isel.pt
Conceição Juana Fortes	LNEC	jfortes@lnec.pt
Rute Lemos	LNEC	rlemos@lnec.pt
Maria Teresa Reis	LNEC	treis@lnec.pt
Rita Carvalho	UCoimbra	ritalmfc@dec.uc.pt
Antje Bornschein	UDresden	antje.bornschein@tu-dresden.de
Moritz Körner	UDresden	koerner.moritz96@icloud.com
Reinhard Pohl	UDresden	reinhard.pohl@tu-dresden.de
Bas Hofland	TU Delft	B.Hofland@tudelft.nl
Jeroen van den Bos	TU Delft	J.P.vandenBos@tudelft.nl
Bastien Dost	UTrier	s6jodost@uni-trier.de
Julius Wimper	UTrier	weimper@uni-trier.de
Oliver Gronz	UTrier	gronz@uni-trier.de
Alberto Alvarellos	UDCoruna	alberto.alvarellos@udc.es
Andrés Figuero	UDCoruna	andres.figuero@udc.es
Enrique Peña	UDCoruna	epena@udc.es
José Sande	UDCoruna	jose.sande@udc.es

## Document History

<b>Date</b>	<b>Status</b>	<b>Author(s)</b>
30.07.2019	Final	João Alfredo Santos, Rute Lemos, Julius Wimper, Oliver Gronz, Bas Hofland, José Sande, Enrique Peña, Maria Teresa Reis, Conceição Juana Fortes, Andrés Figuero, Antje Bornschein, Nils Kerpen, Francisco Pedro, Mário Coimbra, Moritz Körner, Jeroen van den Bos, Bastien Dost, Rita Carvalho, Alberto Alvarellos, Reinhard Pohl

## Document objective

This data storage report describes the project and how data were collected. The data are described so that others can use them.

## Acknowledgement

The work described in this publication was supported by the European Community's Horizon 2020 Research and Innovation Programme through the grant to HYDRALAB-PLUS, Contract no. 654110.

## Disclaimer

This document reflects only the authors' views and not those of the European Community. This work may rely on data from sources external to the HYDRALAB-PLUS project Consortium. Members of the Consortium do not accept liability for loss or damage suffered by any third party as a result of errors or inaccuracies in such data. The information in this document is provided "as is" and no guarantee or warranty is given that the information is fit for any particular purpose. The user thereof uses the information at its sole risk and neither the European Community nor any member of the HYDRALAB-PLUS Consortium is liable for any use that may be made of the information.

## License



<http://creativecommons.org/licenses/by/4.0/>

# Contents

1	Introduction.....	6
1.1	Scientific background.....	6
1.2	Aims and Objectives.....	6
2	Experimental setup.....	8
2.1	General description of experimental setup.....	8
2.2	General data storage principles and organization of data files.....	10
2.3	Definition and application of spatial and temporal reference systems.....	11
2.4	Relevant fixed parameters.....	12
2.5	Test Programme.....	12
3	Instrumentation – Acoustic Wave Gauges (LUHannover).....	14
3.1	Instruments.....	14
3.2	Measured parameters.....	14
3.3	Experimental procedure.....	14
3.4	Data post-processing.....	14
3.5	Organization of data files.....	14
3.6	Remarks.....	14
4	Instrumentation – Acoustic Doppler Velocimeters (LUHannover).....	15
4.1	Instruments.....	15
4.2	Measured parameters.....	15
4.3	Experimental procedure.....	15
4.4	Data post-processing.....	15
4.5	Organization of data files.....	15
4.6	Remarks.....	15
5	Instrumentation – Arrays of Acoustic Wave Gauges (LUHannover).....	16
5.1	Instruments.....	16
5.2	Measured parameters.....	16
5.3	Experimental procedure.....	16
5.4	Data post-processing.....	16
5.5	Organization of data files.....	16
5.6	Remarks.....	17
6	Instrumentation – Capacitive Wave Gauges (LUHannover).....	18
6.1	Instruments.....	18
6.2	Measured parameters.....	18
6.3	Experimental procedure.....	18
6.4	Data post-processing.....	18
6.5	Organization of data files.....	18
6.6	Remarks.....	18
7	Instrumentation – Load Cells (LUHannover).....	19
7.1	Instruments.....	19
7.2	Measured parameters.....	19
7.3	Experimental procedure.....	19
7.4	Data post-processing.....	19
7.5	Organization of data files.....	19
7.6	Remarks.....	19
8	Instrumentation – Photogrammetry Cameras (LNEC).....	20
8.1	Instruments.....	20
8.2	Measured parameters.....	20
8.3	Experimental procedure.....	20
8.4	Data post-processing.....	20
8.5	Organization of data files.....	20
8.6	Remarks.....	21
9	Instrumentation – Smartstones (UTrier).....	22
9.1	Instruments.....	22

9.2	Measured parameters.....	22
9.3	Experimental procedure.....	22
9.4	Data post-processing.....	22
9.5	Organization of data files.....	22
9.6	Remarks .....	23
10	Instrumentation – Smart cubes/Antifers (TUDelft) .....	24
10.1	Instruments .....	24
10.2	Measured parameters.....	24
10.3	Experimental procedure.....	24
10.4	Data post-processing.....	25
10.5	Organization of data files.....	25
10.6	Remarks .....	25
11	Instrumentation – Kinect motion sensor (UdCoruna).....	26
11.1	Instruments .....	26
11.2	Measured parameters.....	26
11.3	Experimental procedure.....	26
11.4	Data post-processing.....	26
11.5	Organization of data files.....	26
11.6	Remarks .....	27
12	Instrumentation – Thermal camera (UdCoruna) .....	28
12.1	Instruments .....	28
12.2	Measured parameters.....	28
12.3	Experimental procedure.....	28
12.4	Data post-processing.....	28
12.5	Organization of data files.....	28
12.6	Remarks .....	28
13	Instrumentation – 3D Laserscan (LUHannover).....	29
13.1	Instruments .....	29
13.2	Measured parameters.....	29
13.3	Experimental procedure.....	29
13.4	Data post-processing.....	29
13.5	Organization of data files.....	29
13.6	Remarks .....	29
14	References .....	30

# 1 Introduction

## 1.1 Scientific background

Global climate change is an assumed scenario for the future. There is an expected impact on the frequency of extreme wind events and of storm surges, as well as of what is now called a sea-wave storm, including changes in the dominant wave direction. However, little is known about the actual failure probability of existing structures under such conditions.

In fact, wave breaking / run-up / overtopping and their impact in the stability of rubble mound breakwaters (both at trunk and roundhead) are not adequately characterized yet for climate change scenarios. The same happens with the influence of high incidence angles in such phenomena, which depend upon experiments in a large-scale set-up.

To ensure an adequate performance for these coastal protection structures in such scenarios without having to increase the breakwaters' dimensions and the associated costs, it is mandatory to understand the influence of angle wave attack on their response in what concerns wave run-up, wave overtopping and hydraulic stability.

Several former investigations on wave run-up and overtopping of (impermeable and permeable) coastal structures aimed at quantifying the influence of oblique waves on mean overtopping discharge, water layer thickness and velocities through the development of empirical formulas of a reduction factor for wave obliquity,  $\gamma_\beta$ . However, most of the formulas did not consider very oblique wave approach.

Regarding the stability of armour layers, especially for very oblique waves, for which the increase in stability is the largest, limited data are available.

Van Gent (2014) performed a set of physical model tests to assess the effects of oblique waves on the stability of rock slopes and of cube armoured rubble mound breakwaters (single and double layers) mostly on a 1:1.5 slope. The physical model tests focussed on wave directions between perpendicular ( $0^\circ$ ) and parallel ( $90^\circ$ ) to the longitudinal structure axis, with long and short-crested waves. A series of test runs were performed with an increasing wave height between 0.025 m to 0.274 m and constant wave steepness of 0.03 or 0.04 (only for a few tests).

Van Gent (2014) recommends the study of the influence of oblique wave attack on the stability of rubble mound structures for: a) other slope angles, especially gentler rock slopes; b) other values of wave steepness, to cover values of the surf similarity parameter outside the range of 2.2-3.5 for rock and 3-3.5 for cubes; c) interlocking armour units.

The tests dealt mainly with recommendations a) and b) and they required a large wave basin to build the model of a multi-layer rubble mound breakwater that included both the breakwater head and the neighbouring trunk, where the effect of the wave attack angle is more important. The wave basin at LUH has a test area that is 30 m long, 15 m wide and 1 m deep, which allows the construction of a large size model, thus reducing the scale effects associated to the wave induced flow across small models.

## 1.2 Aims and Objectives

The gaps in existing data and the R&D&I experience of the team members on wave run-up and overtopping, on damage in rubble mound breakwaters and on different techniques to assess the motion of their armour layer elements, triggered the common interest in developing the present experimental work. Its main goal is to contribute to a new whole understanding of the phenomena to mitigate future sea level rise in European coastal structures, including the run-up and overtopping characterization on rough and permeable slopes, as well as to check and extend the validity range of the formulas developed for armour layer stability.

To ensure an adequate performance for rubble-mound breakwaters in climate change scenarios without having to increase the breakwaters' dimensions and the associated costs, it is mandatory to understand the influence of angle wave attack on their response in what concerns wave run-up, wave overtopping and hydraulic stability. Therefore, the results from these tests will also help in assessing

design and maintenance strategies to increase the lifespan and resilience of rubble-mound breakwaters, reducing monetary costs for re-construction and climate change adaptation.

So, the proposed experiment will provide a set of data for engineering and economic better decision-making processes:

- Extend or improve the validity range of the available empirical formulas (Van Gent, 2014; Macineira & Burcharth, 2016) for armour layer stability (wave steepness and obliquity), both at the trunk and roundhead, which will enable the assessment of existing structures performance in climate change scenarios;
- Calibrate and validate empirical formulas for wave run-up and overtopping, as well as IHFOAM simulations, in climate change scenarios, which will enable to reduce risks to pedestrians, goods and infrastructure in ports.

This experiment was also a unique scientific opportunity to assess and improve some of the non-intrusive techniques developed by the team members to measure quantities related to armour layer damage, namely: a) the digital stereo photography methods Pedro et al. (2015) for the survey of the armour layer envelope; d) the Smartstones of Gronz et al. (2016) and the smart cubes developed at TUDelft (Hofland et al. 2018).

## 2 Experimental setup

### 2.1 General description of experimental setup

A stretch of a rubble mound breakwater (head and part of the adjoining trunk, with a slope of 1(V):2(H)) was built in the wave basin of the Leibnitz Universität Hannover. Since the incidence angles to be tested ranged from  $40^\circ$  to  $90^\circ$  (wave direction parallel to the model axis) the model was built with its axis making an angle of  $70^\circ$  to the tank wall opposite the wave maker.

Figure 2-1 presents the plan view of the breakwater model as well as a cross section that passes through the overtopping tank closest to the breakwater head. As it can be seen in the figure the trunk of the breakwater is 7.5 m long and the head has the same cross section as the exposed part of breakwater. The total model length, measured along the crest axis, is 9.3 m, the model height is 0,83 m and its width is 3.7 m.

The armour layer of the breakwater head, as well as of the 2.5 m wide adjoining exposed strip, was made of two layers of 351 gf Antifer cubes. The remaining 5 m of the breakwater trunk had an armour layer made of rock (gravel) with a median weight of 315 gf. It must be pointed out that the same rock was employed also in the 7.5 m of armour layer at the lee side of the breakwater. It was expected that the porosity of the armour layer was 37%. The filter layer was made of gravel with a median weight of 59 gf whereas the toe was made of gravel with a median weight of 260 gf. The core was made of gravel with a median weight of 6 gf. A cross section of the breakwater trunk is presented in Figure 2-2.

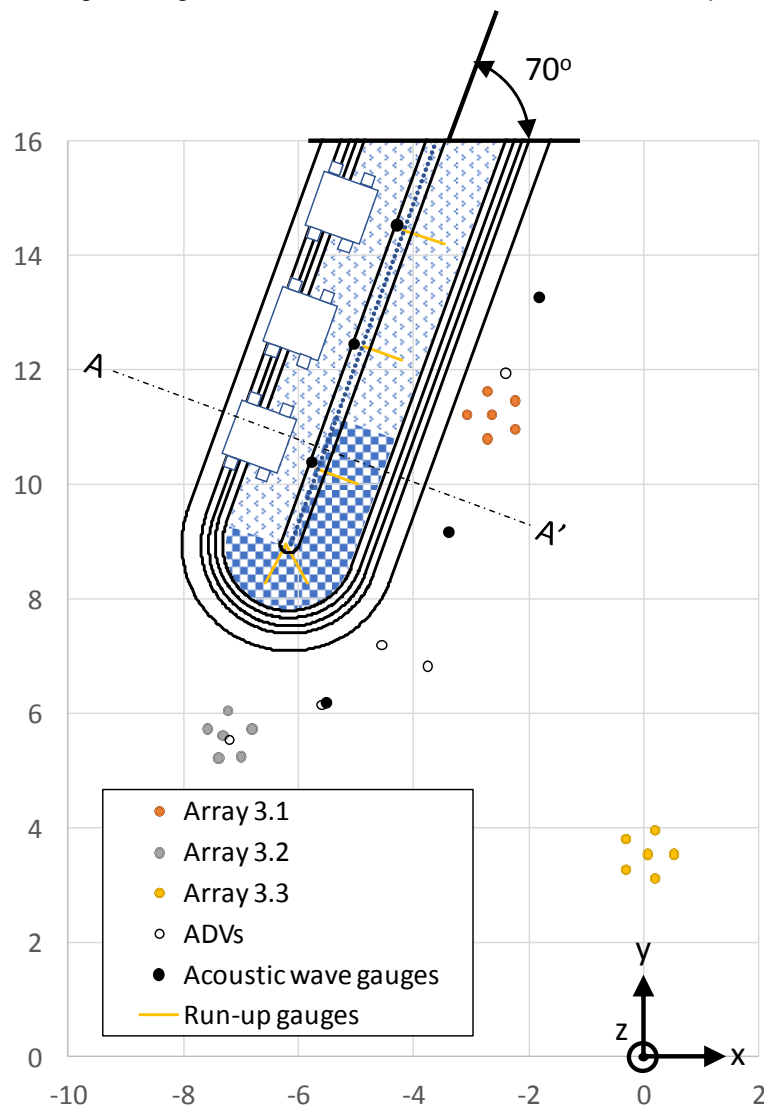
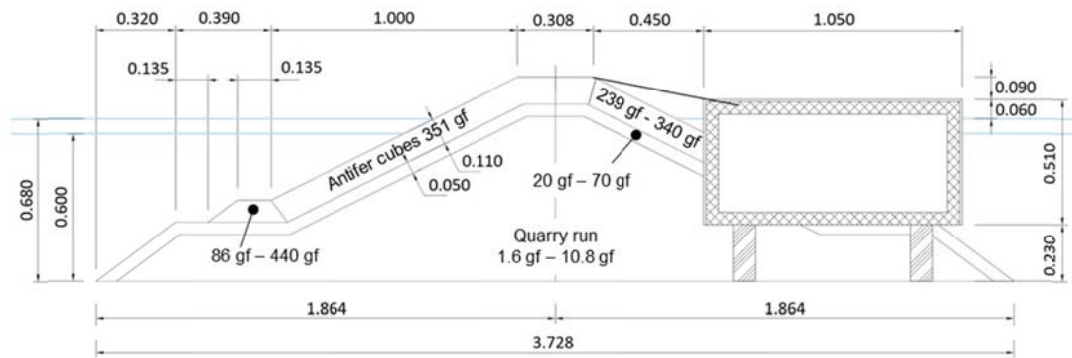


Figure 2-1. Plan view of the the experimental setup.





**Figure 2-2.** Cross section of the breakwater.

The trunk core was built using plywood moulds that were left inside the structure. No core moulds were left at the breakwater head.

Four different categories can be identified in the equipment deployed in the experiment according to the variables measured:

- Sea waves
  - three arrays of six acoustic wave probes (3.x.y) (x=1 to 3; y=1 to 6);
  - three isolated acoustic wave probes (1.1.x) (x=1 to 3);
  - five ADV - acoustic Doppler velocimeters (2.x) (x=1 to 5)
- Run-up
  - five capacitive wave gauges, 0.87 m long, (4.1.x) (x=1 to 5)
  - one thermal camera placed on top of the trunk part with Antifer cubes in the armour layer
- Overtopping;
  - Three 500 l overtopping reservoirs
  - One load cell beneath each reservoir to weigh the overtopped volume (5.x) (x=1 to 3)
  - One acoustic wave gauge in front of the entrance of the chute, to identify overtopping events (1.2.x) (x=1 to 3)
  - One capacitive wave gauge inside the overtopping tank to have redundancy in the measurement of the overtopped volume (4.2.x) (x=1 to 3)
- Armour layer damage.
  - stereo photogrammetry
  - Kinect motion sensor
  - 6 Antifer cubes with accelerometers inside them

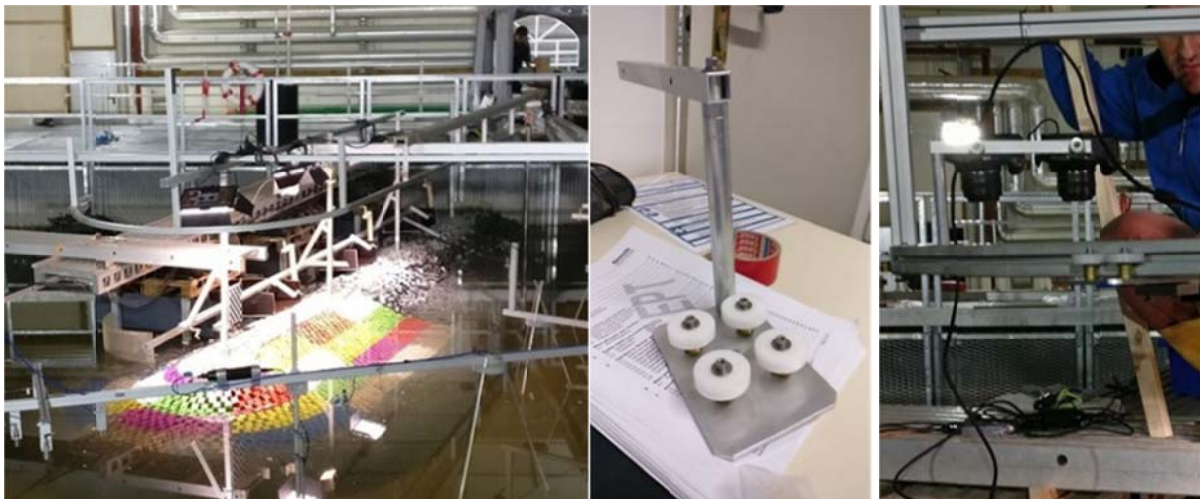
A plan view of the key instruments for those variables (apart from “armour layer damage”) is presented on Figure 2-1. The numbering of the instruments (x) increased from the breakwater root to the breakwater head.

Figure 2-3 presents a view of the general layout at the entrance of overtopping reservoir 1, the one closest to the breakwater root. The chute to carry overtopped water into the overtopping tank, as well as the acoustic wave gauge to identify overtopping events can be seen there. The run-up gauges on the breakwater trunk were placed close to the overtopping measuring section, hence the run-up gauge in the figure.



**Figure 2-3.** General layout at the entrance of an overtopping reservoir (run-up wave gauge and acoustic wave gauge to identify overtopping events).

The first two techniques for measuring armour layer damage implied the movement of equipment above the study region. So, an aluminium rail made of a straight stretch 7.85 m long and of a semi-circumference stretch with a diameter of 1.80 m was hung 2.00 m above the wave basin bottom (Figure 2-4).



**Figure 2-4.** Left: rail to support the photographic cameras and the Kinect motion sensor; Middle: wagon to carry those cameras; Right: wagon on the rail with two cameras.

A laser scan survey of the armour layer envelope established the ground truth for the measurements made with those two techniques. This was done at the second day of tests, just before the beginning of the test series and at the end of that test series. The same happened with the last test series.

Not all equipment was available for the whole duration of the tests. The Kinect motion sensor was brought by the UdCoruna team and taken with them at the end of test\_039 (day 06 of tests, 2017-11-08). The Smartifers brought by the TUDelft team were available until the end of test\_044 (day 07 of tests, 2017-11-09) whereas the smartstones brought by the UTrier team were available until the end of test\_48 (day 08 of tests, 2017-11-10).

## 2.2 General data storage principles and organization of data files

Data was stored per testing day. See test sequence in 2.5. The major reason for that it was the need to collect each day information for the calibration of the stereo photogrammetry procedure, namely the cameras intrinsic parameters and the definition of the air-water interface position.

For each day, there is

- **photogrammetry\_calibration** with the two subfolders
  - **camera\_parameters**, with jpg files of the image pairs of a chequered plate of known dimensions, needed to define the intrinsic cameras' parameters as well as the parameters of the pair of cameras;
  - **still\_water\_level**, with the jpg files of the image pairs of the same chequered plate now placed at the free-surface;

And then the data from each test with serial number nnn is stored in the folder

**Test\_nnn**, with five subfolders at most

- **before\_filling**, only for the first test of the day, with the survey of the dry armour layer envelope of the undamaged / rebuilt breakwater, before water being put in the wave tank, with three subfolders at most
  - **photogrammetry\_LNEC**, with the jpg files of the image pairs taken at four points along the breakwater;
  - **dry\_before\_Tnnn\_Kinect\_UdCoruna.7z**, with the ply files obtained from the Kinect surveys taken at 20 plus points along the breakwater head;
  - **laserscan\_LUHannover**, with the files obtained from the laserscan surveys
- **beginning**, only for the first test of the day, after the water level being set for the tests, again with the undamaged / rebuilt breakwater, to assess the ability of the surveying procedures to compensate for the presence of the air-water interface. With two subfolders at most
  - **photogrammetry\_LNEC**, with the jpg files of the image pairs taken at four points along the breakwater;
  - **before\_Tnnn\_Kinect\_UdCoruna.7z**, with the ply files obtained from the Kinect surveys taken at 20 plus points along the breakwater head;
- **during**, with the data collected during the test, i.e the files
  - **Tnnn\_mostly\_free\_surface\_elevation\_LUHannover.txt**, with free-surface elevation data measured in the wave tank, as well as the runup and overtopping data
  - **Tnnn\_2\_x\_YYYYMMDDhhmmss\_ADV\_LUHannover.vna**, with the data collected at ADV x, one file per ADV
  - **Tnnn\_sss\_Stone\_UTrier.csv**, with the data collected at the smartstone sss;
  - **Tnnn\_Cubea\_TUDelft.mat**, with the data collected at the smart cube a;
  - **Tnnn\_thermal\_UdCoruna.7z** with the PNG files with the thermal camera images
- **end**, with the surveys of the armour layer envelope after the action of the incident sea waves. Two subfolders at most
  - **photogrammetry\_LNEC**, with the jpg files of the image pairs taken at four points along the breakwater;
  - **Tnnn\_Kinect\_UdCoruna.7z**, with the ply files obtained from the Kinect surveys taken at 20 plus points along the breakwater head;
- **Tank\_empty\_end**, only for the last test of the day with the survey of the dry armour layer envelope of the damaged breakwater, after water being removed from the wave tank, with three subfolders at most
  - **photogrammetry\_LNEC**, with the jpg files of the image pairs taken at four points along the breakwater;
  - **Tnnn\_dry\_Kinect\_UdCoruna.7z**, with the ply files obtained from the Kinect surveys taken at 20 plus points along the breakwater head;
  - **laserscan\_LUHannover**, with the files obtained from the laserscan surveys

### 2.3 Definition and application of spatial and temporal reference systems

All space coordinates are relative to a reference system placed on the bottom of the wave tank in front of the middle of the paddle row of the wave maker, as can be seen in Figure 2-1. Detailed information on the coordinates of some instruments is given in their corresponding chapters.

No temporal reference system was used.

## 2.4 Relevant fixed parameters

No relevant fixed parameters

## 2.5 Test Programme

Two water levels (0.60 m and 0.68 m), five wave incidence angles to the normal to the breakwater axis ( $40^\circ$ ,  $55^\circ$ ,  $65^\circ$ ,  $75^\circ$  and  $90^\circ$ ) and four sea-wave conditions, with a wave steepness of 0.055 were tested ( $H_s = 0.100$  m, 0.150 m, 0.175 m and 0.200 m and the corresponding peak periods  $T_p = 1.19$  s, 1.45 s, 1.57 s and 1.68 s). Tests were carried out with long-crested (most of them) and short crested waves. The duration of each test was meant to correspond to 1000 waves.

One test sequence was carried out per working day and it consisted of one wave direction, one water depth and four incident sea-waves with growing significant wave height and the same wave steepness of 0.055. At the end of the test sequence the armour layer was rebuilt, i.e. the displaced armour elements were put back in their initial positions.

There was a quite complete sweep of wave incidence angles for long-crested waves and the water depth of 0.60 m ( $40^\circ$ ,  $55^\circ$ ,  $65^\circ$ ,  $75^\circ$  and  $90^\circ$ ).

Since it was expected that no major run-up, overtopping or damage would occur along the structure for high incidence angles, in the test series with the water depth of 0.68 m and long-crested waves, the number of incidence angles was reduced. Only 3 different angles were considered ( $40^\circ$ ,  $55^\circ$  and  $65^\circ$ ).

The influence of the directional spreading of short-crested waves was investigated for the lowest water depth (0.60 m) and the incidence angles of  $40^\circ$  and  $65^\circ$ . These are the mean directions of the peak period and the directional spreading tested was  $50^\circ$ .

Finally, for the incidence angle of  $40^\circ$  results were also obtained for the highest water depth (0.68 m) and short-crested waves with a directional spreading of  $50^\circ$ .

To test the repeatability of the wave maker, on 2017-11-13, there were four repeats of test\_049, i.e. Test\_054, Test\_055, Test\_056 and Test\_057. Test\_053 was aborted because a wrong file was used to control the wave maker. There was a survey of the armour layer envelope at the end of Test\_052 and another at the end of Test\_057, only.

In the last testing day, 2017-11-15, the test carried out with the highest sea state, Test\_068, was repeated four times: Test\_069, Test\_070, Test\_071 and Test\_072. In the last test it was decided to remove the runup gauges at the breakwater roundhead, 4.1.4 and 4.1.5. As before, there was a survey of the armour layer envelope after Test\_068 and another after Test\_072.

The sequence of folders and subfolders in 2.3 gives a good idea on data collected before the test sequence started, both without and with water in the wave basin, then what was collected during and after each test, as well as after the of the test sequence, with an empty wave basin. The most relevant exception is related to the laserscan surveys. Only four were carried out, all with the empty tank: they happened before and after the test sequence of testing day 2, 2017-11-02, and of day 11, 2017-11-15.

**Table 2-1.** Test parameters.

Date	Test	d (m)	Hm0 (m)	Tp (s)	Dir (°)	Spread (°)
01-11-2017	13	0.60	0.100	1.19	40	0
	14		0.150	1.45		
	15		0.175	1.57		
	16		0.200	1.68		
02-11-2017	17	0.60	0.100	1.19	65	0
	18		0.150	1.45		
	19		0.175	1.57		
	20		0.200	1.68		
03-11-2017	21	0.60	0.100	1.19	90	0
	22		0.150	1.45		
	23		0.175	1.57		
	25		0.200	1.68		
06-11-2017	26	0.68	0.250	1.88	40	0
	27		0.100	1.19		
	28		0.150	1.45		
	29		0.175	1.57		
07-11-2017	30	0.68	0.200	1.68	65	0
	31		0.100	1.19		
	32		0.150	1.45		
	33		0.175	1.57		
08-11-2017	34	0.60	0.200	1.68	40	50
	35		0.100	1.19		
	36		0.150	1.45		
	37		0.175	1.57		
09-11-2017	38	0.60	0.200	1.68	65	50
	39		0.250	1.88		
	40		0.100	1.19		
	41		0.150	1.45		
10-11-2017	42	0.60	0.175	1.57	55	0
	43		0.200	1.68		
	44		0.250	1.88		
	45		0.100	1.19		
13-11-2017	46	0.60	0.150	1.45	75	0
	47		0.175	1.57		
	48		0.200	1.68		
	49		0.100	1.19		
14-11-2017	50	0.68	0.150	1.45	55	0
	51		0.175	1.57		
	52		0.200	1.68		
	58		0.100	1.19		
15-11-2017	59	0.68	0.150	1.45	40	50
	60		0.175	1.57		
	61		0.200	1.68		
	63		0.250	1.88		
	64	0.68	0.100	1.19	40	50
	65		0.150	1.45		
	66		0.175	1.57		
	67		0.200	1.68		
	68		0.250	1.88		

### 3 Instrumentation – Acoustic Wave Gauges (LUHannover)

#### 3.1 Instruments

6 standalone acoustic wave gauges connected to HBM Catman data acquisition device.

#### 3.2 Measured parameters

Free-surface elevation (m) is obtained from the deviation from an initial position that is estimated from the time taken by reflected sound wave to return to the emitting gauge.

#### 3.3 Experimental procedure

3 acoustic wave gauges (1.1.1 to 1.1.3) were deployed in the wave tank at the positions shown in Table 3-1 to get point measurements of free-surface elevation. Another 3 (1.2.1 to 1.2.3) were deployed over the chute that takes overtopped water into the overtopping reservoir 1 to 3, respectively, to identify overtopping events.

**Table 3-1.** Coordinates of the standalone acoustic wave gauges.

probe	x(m)	y(m)
1.1.1	-1.82	13.31
1.1.2	-3.39	9.19
1.1.3	-5.50	6.20

The sampling rate was 300 Hz. All these measurements were synchronized and were carried out for all the tests.

#### 3.4 Data post-processing

Provided datasets contain raw data without post-processing.

#### 3.5 Organization of data files

Format: .txt

File name: Tnnn\_mostly\_free\_surface\_elevation\_LUHannover.txt, nnn being test number

38 initial rows with general information on the data acquisition

data in columns:

columns 1, 17 and 26: time (s) from the start of recording

columns 8 to 10: free-surface elevation (m) measured in the wave tank at wave gauges 1.1.1 to 1.1.3, respectively

columns 27 to 29: free-surface elevation (m) above chute that leads to the overtopping reservoir (1.2.1 to 1.2.3, respectively)

Organization of files in directories: each file is stored in the corresponding test\_nnnn\during directory

#### 3.6 Remarks

The data file contains measurements from other transducers, mostly related with free-surface elevation, including run-up and overtopping. They are all synchronized with the 300 Hz sampling rate. There was no synchronization between these measurements and the ADV ones, which were carried out with 100 Hz sampling rate.

## 4 Instrumentation – Acoustic Doppler Velocimeters (LUHannover)

### 4.1 Instruments

5 Nortek's acoustic doppler velocimeters (code-named 2.1 to 2.5) deployed in the wave tank and connected directly to the communication port of one personal computer.

### 4.2 Measured parameters

3 components (x,y,z) of the particles velocity (m/s) in vertical cylindrical region with a diameter of 6 mm and a height of 10 mm that lies 50 mm below the acoustic transmitter of the ADV.

### 4.3 Experimental procedure

The ADVs were deployed in the wave tank such that the position of the acoustic transmitter of each ADV is the one presented in Table 4-1. The acoustic receiver that defines the x axis was aligned with the breakwater crest in all ADVs.

**Table 4-1.** Coordinates of the acoustic transmitter of the ADV.

ADV	x(m)	y(m)	z(m)
2.1	-2.40	11.96	0.40
2.2	-5.58	6.16	0.40
2.3	-7.20	5.56	0.41
2.4	-3.75	6.83	0.29
2.5	-4.55	7.20	0.11

The sampling rate was 300 Hz. All the ADV measurements were synchronized and were carried out for all the tests.

### 4.4 Data post-processing

Provided datasets contain raw data without post-processing.

### 4.5 Organization of data files

Format: .vna

File name: Tnnn\_2\_x\_yyyyMMddhhmm\_ADV\_LUHannover.vna, nnn being test number, x ADV number, yyyy year, MM month, dd day, hh hour, mm minute

data in columns:

column 2: time (s) from the start of recording

column 5: x component of velocity (m/s)

column 6: y component of velocity (m/s)

column 7: z component of velocity (m/s)

Organization of files in directories: the files are stored in the corresponding test\_nnnn\during directory

### 4.6 Remarks

The sampling rate used in the ADVs was different from the one in the remaining instruments used to characterize sea-waves in the experiments, 300 Hz. There was no synchronization of the ADVs measurements and the ones from those instruments.

## 5 Instrumentation – Arrays of Acoustic Wave Gauges (LUHannover)

### 5.1 Instruments

3 arrays made of 6 acoustic wave gauges connected to HBM Catman data acquisition device.

### 5.2 Measured parameters

Free-surface elevation (m) is obtained from the deviation from an initial position that is estimated from the time taken by reflected sound wave to return to the emitting gauge.

### 5.3 Experimental procedure

Each set of 6 acoustic wave gauges (3.1 to 3.3) was deployed in the wave tank at the positions shown in Table 5-1 to get simultaneous measurements of free-surface elevation. Array 3.1 was in front of the middle of the trunk; array 3.2 was in front of the roundhead; array 3.3 was in front of the wavemaker.

**Table 5-1.** Coordinates of the acoustic probes in the wave gauge arrays.

Array	probe	x(m)	y(m)
3.1	3.1.1	-2.71	11.65
	3.1.2	-3.05	11.23
	3.1.3	-2.70	10.80
	3.1.4	-2.23	10.98
	3.1.5	-2.22	11.48
	3.1.6	-2.64	11.23
3.2	3.2.1	-7.55	5.75
	3.2.2	-7.39	5.24
	3.2.3	-6.99	5.26
	3.2.4	-6.80	5.75
	3.2.5	-7.23	6.06
	3.2.6	-7.29	5.63
3.3	3.3.1	-0.29	3.82
	3.3.2	-0.29	3.30
	3.3.3	0.21	3.14
	3.3.4	0.52	3.56
	3.3.5	0.22	3.99
	3.3.6	0.08	3.56

The sampling rate was 300 Hz. All these measurements were synchronized and were carried out for all the tests.

### 5.4 Data post-processing

Provided datasets contain raw data without post-processing. The 6 simultaneous measurements of the free-surface elevation will enable the estimation of the directional wave spectrum at that region.

### 5.5 Organization of data files

Format: .txt

File name: Tnnn\_mostly\_free\_surface\_elevation\_LUHannover.txt, nnn being test number

38 initial rows with general information on the data acquisition

data in columns:

data in columns:

columns 1, 17 and 26: time (s) from the start of recording



columns 33 to 38: free-surface elevation (m) measured at wave gauges 3.1.1 to 3.1.6, respectively

columns 11 to 16: free-surface elevation (m) measured at wave gauges 3.2.1 to 3.2.6, respectively

columns 2 to 7: free-surface elevation (m) measured at wave gauges 3.3.1 to 3.3.6, respectively

Organization of files in directories: each file is stored in the corresponding test\_nnnn\during directory

## **5.6 Remarks**

The data file contains measurements from other transducers, mostly related with free-surface elevation, including run-up and overtopping. They are all synchronized with the 300 Hz sampling rate. There was no synchronization between these measurements and the ADV ones, which were carried out with 100 Hz sampling rate.

## 6 Instrumentation – Capacitive Wave Gauges (LUHannover)

### 6.1 Instruments

8 capacitive wave gauges connected to HBM Catman data acquisition device. 5 wave gauges had a length of approximately 60 cm and 3 a length of 50 cm.

### 6.2 Measured parameters

Length (mm) of the submerged part of the probe is estimated from the changes in the electric current resulting from the variation of the electric capacitance of water between the two terminals of the probe.

### 6.3 Experimental procedure

The long wave gauges (4.1.1. to 4.1.5) were used to measure wave runup. They were deployed over the armour layer such that their extremities had the coordinates presented in table xx. Each of the remaining 3 (4.2.1 to 4.2.3) was placed inside the overtopping reservoir 1 to 3, respectively, to measure the increase of the water level there due to overtopping.

**Table 6-1.** Coordinates of the extremities of the runup gauges.

Run up gauge	Top			Bottom		
	X	y	Z	x	y	Z
4.1.1	--4.14	14.43	1.00	-3.45	14.18	0.54
4.1.2	-4.85	12.40	1.02	-4.17	12.16	0.54
4.1.3	-5.66	10.26	1.02	-4.95	10.00	0.60
4.1.4	-6.25	8.81	0.90	-6.58	8.25	0.57
4.1.5	-6.16	8.89	0.95	-5.82	8.27	0.61

The sampling rate was 300 Hz. All these measurements were synchronized and were carried out for all the tests.

### 6.4 Data post-processing

Provided datasets contain raw data without post-processing.

### 6.5 Organization of data files

Format: .txt

File name: Tnnn\_mostly\_free\_surface\_elevation\_LUHannover.txt, nnn being test number

38 initial rows with general information on the data acquisition

data in columns:

columns 1, 17 and 26: time (s) from the start of recording

columns 18 to 22: runup (mm) measured at wave gauges 4.1.1 to 4.1.5, respectively

columns 30 to 32: free-surface elevation (mm) measured at wave gauges 4.2.1 to 4.2.3 placed, respectively, inside overtopping reservoir 1 to 3

Organization of files in directories: each file is stored in the corresponding test\_nnnn\during directory

### 6.6 Remarks

The data file contains measurements from other transducers, mostly related with free-surface elevation and overtopping. They are all synchronized with the 300 Hz sampling rate. There was no synchronization between these measurements and the ADV ones, which were carried out with 100 Hz sampling rate.

## **7 Instrumentation – Load Cells (LUHannover)**

### **7.1 Instruments**

3 load cells connected to HBM Catman data acquisition device.

### **7.2 Measured parameters**

Weight (kgf) of the overtopped volume inside the corresponding overtopping reservoir.

### **7.3 Experimental procedure**

Each overtopping reservoir had a capacity of 500 l and was placed inside a watertight container. The water volume inside each overtopping reservoir was weighted with a load cell placed between the bottom of that reservoir and its container. A trapezoidal chute 0.60 m long and an entrance width of 0.60 m (and an exit width of 0.50 m) conveyed the overtopped water volume from the inner edge of the breakwater crest into the reservoir.

The sampling rate was 300 Hz. All these measurements were synchronized and were carried out for all the tests.

### **7.4 Data post-processing**

Provided datasets contain raw data without post-processing.

### **7.5 Organization of data files**

Format: .txt

File name: Tnnn\_mostly\_free\_surface\_elevation\_LUHannover.txt, nnn being test number

38 initial rows with general information on the data acquisition

data in columns:

columns 1, 17 and 26: time (s) from the start of recording

columns 23 to 25: weight (kgf) measured at load cell 5.1 to 5.3 placed, respectively between the overtopping reservoir 1 to 3 and the corresponding container

Organization of files in directories: each file is stored in the corresponding test\_nnnn\during directory

### **7.6 Remarks**

The data file contains measurements from other transducers, mostly related with free-surface elevation and run-up. They are all synchronized with the 300 Hz sampling rate. There was no synchronization between these measurements and the ADV ones, which were carried out with 100 Hz sampling rate.

## 8 Instrumentation – Photogrammetry Cameras (LNEC)

### 8.1 Instruments

Two digital SLR cameras (Canon EOS 600D) fitted common remote trigger

Fixed focal length lenses (Canon EF 35mm  $f/2$ ),

Aluminium rail 2,0 m above the wave tank bottom.

Checkered target for camera calibration

### 8.2 Measured parameters

Three-dimensional coordinates (m) of point clouds resulting from photogrammetric survey.

### 8.3 Experimental procedure

Two digital SLR cameras (Canon EOS 600D) fitted with fixed focal length lenses (Canon EF 35mm  $f/2$ ) were mounted side by side in a carriage that travelled along the support structure, approximately 2,0 m above the tank bottom; they were triggered with a common remote at 4 positions along the breakwater: one position over the region containing the entrance of each overtopping reservoir and one position over the breakwater head along the breakwater crest. Photogrammetric surveys were conducted for Tests 13 to 72.

### 8.4 Data post-processing

Provided datasets contain raw data without post-processing.

### 8.5 Organization of data files

Format: .JPG

File name: context\_region\_LNEC\_img\_ssss\_h.jpg,

h a character indicating the side of the image pair (l – left hand side image / r – right hand side image);

ssss being the serial number of the image file,

region designates the part of the structure where the image was taken (trunk\_1, trunk\_2, trunk\_3 or head);

context explains how the image was taken

cal\_yyyy\_mm\_dd or SWL\_yyyy\_mm\_dd, yyyy being the year, mm the month and dd the day  
dry\_before\_Tnnn, before\_Tnnn, Tnnn or Tnnn\_dry, nnn being the test number

Type of data: image files

Units of data: n/a

Structure of file content: each file has 2592 x 1728 pixels

Organization of files in directories: both left and right images are stored at the same subfolder region, which is hanging on folder/subfolder sequence that depends on the context above

yyyy-dd-mm\calibration\_photogrammetry\camera\_parameters\region, if context is cal\_yyyy\_mm\_dd

yyyy-dd-mm\calibration\_photogrammetry\air\_water\_interface\_definition\region, if context is SWL\_yyyy\_mm\_dd

yyyy-nn-dd\Test\_nnn\before\_filling\region, if context is dry\_before\_Tnnn

yyyy-nn-dd\Test\_nnn\beginning\region, if context is before\_Tnnn

yyyy-nn-dd\Test\_nnn\end\region, if context is Tnnn

yyyy-nn-dd\Test\_nnn\tank\_empty\_end\region, if context is Tnnn\_dry

## **8.6 Remarks**

None.

## 9 Instrumentation – Smartstones (UTrier)

### 9.1 Instruments

6 Smartstone probes, each combines a 3-axis accelerometer, 3-axis gyroscope (Bosch Sensortec BMI160) and 3 axis geomagnetic sensor (Bosch Sensortec BMM150), temperature sensor, on-board data storage, RFID antenna, control unit.

1 USB-Gateway for data transmission via RFID to a notebook computer.

6 marked armour units (antifer cubes) with boreholes to fit Smartstone probes into the Antifer cubes.

Custom Software SST GUI I9003.

### 9.2 Measured parameters

3-axial acceleration and 3-axial angular velocity of instrumented armour units.

### 9.3 Experimental procedure

Smartstones were inserted into the marked armour units. Instrumented units were placed in the armour layer at the roundhead of the breakwater, close to the waterline before each set of tests. Smartstones were set to measurement mode at the beginning of each test to record data during the tests. Following each test, data was read out from each active Smartstone via wireless transmission and stored on the hard disk of the notebook.

Smartstones were used during 35 tests, with a minimum of one and a maximum of six Smartstones for one individual test.

### 9.4 Data post-processing

Provided datasets contain raw data without post-processing.

### 9.5 Organization of data files

Format: .csv

File name: Tnnn\_sss\_Stone\_Utrier.csv; nnn being the test number and sss a three-digit with the sensor ID

Type of data: Comma-separated text

Units of data: ms, g, °/s

Structure of file content:

header-line: internal sensor number, software version

data in columns:

column 1: flag related to trigger of recording,

column 2 time in ms,

column 3: angular velocity x-axis

column 4: angular velocity y-axis

column 5: angular velocity z-axis

column 6: acceleration x-axis

column 7: acceleration y-axis

column 8: acceleration z-axis

Organization of files in directories: each file is stored in the corresponding test\_nnnn\during directory

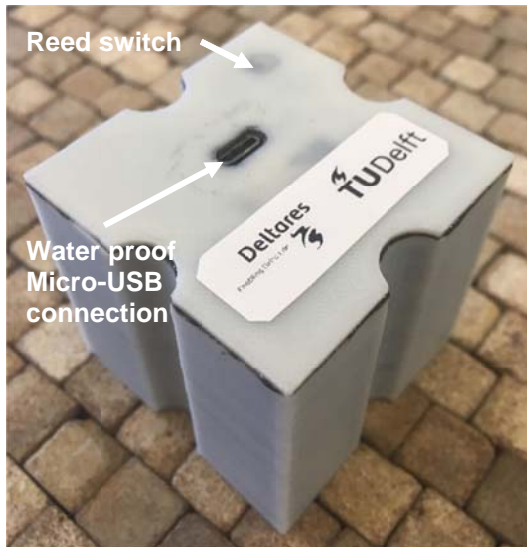
## **9.6 Remarks**

The Smartstone probe is a prototype, not a commercial product. It is currently under development. Measurements were made from 2017-11-01 to 2017-11-10.

## 10 Instrumentation – Smart cubes/Antifers (TUDelft)

### 10.1 Instruments

Three 3D-printed antifer cubes, with the same dimensions and weight as the other cubes in the breakwater armour. Inside are a small Arduino computer that includes processing board, 9-axis IMU, battery, SD card, and water proof Micro-USB connection, reed switch to switch the sensor off. See photos below.



### 10.2 Measured parameters

Three-components of acceleration (including gravitational acceleration) [G] and angular velocity [rad/s]. The sensor axis orientations vary per cube, but can be inferred from the static readings of G, and the fact that they were initially always placed on the slope with the same orientation (see figure above).

### 10.3 Experimental procedure

Start with empty SD card

Connect Antifer unit to computer via USB cable

Run tud\_Sensor2SD on the Arduino ODE. This configures the SD card (if needed) and starts the measurements.

Remove USB after setup has been completed (when prompted through the serial monitor)

Place magnet on the reed-sensor (magnetic sensor) in the corner of the cube(s) to switch the power off and stop sampling.

Place the cube(s) in the breakwater.

Prior to the test: remove magnet from the reed-sensor (magnetic sensor) in the corner of the cube(s) to switch the power on and sampling will automatically begin.

Measurements are written to SD card at approximately 30 Hz. Name of the data file is "datalog.txt".

Measurements are now running.

When power is disconnected during measurements, measurements are resumed when power is reconnected. At that moment a new header line ("starting new measurements...") is printed on the SD card and the data output is resumed below that line, all in the same file. No new file is opened.

After each test: add magnet to reed-sensor (magnetic sensor) in the corner to switch the power off, create a header and save battery life.



After ca. 4 tests remove cube from breakwater, read out the data, clean the SD card, and charge cube via USB.

## 10.4 Data post-processing

As typically all tests performed on one day were stored in the cubes, the raw data that was read out each day consisted of one long list of numbers, that was interrupted by headers that were generated if the sensor was switched off (by placing a magnet on the internal switch) in between the tests. The postprocessing that was performed was cutting the tests into pieces belonging to the specific tests and saving them as MATLAB files per test (and cube).

## 10.5 Organization of data files

What is provided is the final data per test stored as a .mat file (per cube). Each file contains the raw data vectors  $dT$ ,  $ax$ ,  $ay$ ,  $az$ ,  $gx$ ,  $gy$  and  $gz$ , as well as a reconstructed time vector  $T$  starting at  $T = 0$  at the beginning of the test. This data can be used for further postprocessing.

The time is in milliseconds. The measured linear accelerations ( $ax$ ,  $ay$ ,  $az$ ), in units of  $g$  [ $m/s^2$ ], and the last three columns contain the measured angular accelerations ( $gx$ ,  $gy$ ,  $gz$ ). The units of the angular acceleration are presently assumed to be radians/s, but further calibration is still required to verify this.

The resulting timeseries per day were cut into segments representing the individual tests. In most of the cases, a day could be clearly cut into four (or five) tests, with the exception of the following:

T013-T016 cube 3: contains only three tests. Probably battery expired halfway through penultimate test (T015) and T016 is missing. Or, alternatively, the magnet switch malfunctioned during T015 and the last recorded test is actually T016. Since we cannot tell, we have only stored the data for T013 and T014.

T013-T016 cube 4: apparently malfunctioning cube, no data for this cube for this day

T021-T026b cube 3: datafile contains only data for what is clearly T025-T026b, apparently T021-T023 are missing for unknown reasons.

T027-T030 cube 1: battery expired halfway through test T029, consequently only T027-T028 stored

T027-T030 cube 3: battery expired halfway through test T030, consequently only T027-T029 stored

T027-T030 cube 3: battery expired just before test T030, consequently only T027-T029 stored

T035-T039 cube 3: also contains the T031-T034 from the day before, SD card was not properly cleared

T035-T039 cube 4: also contains the T031-T034 from the day before, SD card was not properly cleared

File name: Tnnn\_CubeA\_TUDeltft.mat, A being the serial digit of the smart cube

Organization of files in directories: the files are stored in the corresponding test\_nnnn\during directory

## 10.6 Remarks

Cube 2 was malfunctioning from the beginning. Cube 1 was malfunctioning halfway the testing programme.

Measurements were made from 2017-11-01 to 2017-11-09.

## 11 Instrumentation – Kinect motion sensor (UdCoruna)

### 11.1 Instruments

Two Kinect camera model One and 2.0

Software Kscan 3D.

### 11.2 Measured parameters

3 D coordinates (m) of the armour layer envelope, which enables one to infer on damage occurred during the test.

### 11.3 Experimental procedure

The Kinect obtained point clouds from the breakwater roundhead dike before and after each test, without having to empty the water in the wave tank after each test.

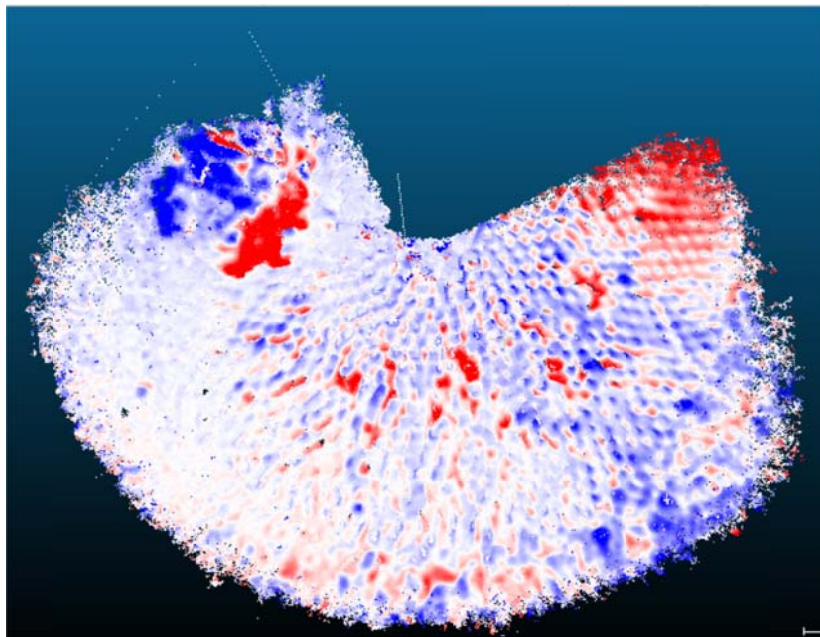
In order to obtain a complete scan of the roundhead, 30 scans are made with a large overlap so that the Kscan 3D program can align them.

### 11.4 Data post-processing

The results can be processed with the Cloud-Compare program. For this purpose, point clouds for two consecutive tests using a program algorithm (M3C2 distances) can be produced.

From it is possible to measure the number of fallen pieces and even the evolution of porosity.

The next figure shows a result obtained in the roundhead. The red color represents erosion and the blue color accretion.



Provided datasets contain ply files without further post-processing.

### 11.5 Organization of data files

Format: .7z

File name: context\_Kinect\_UdCoruna.7z;

context explains how the data was obtained: dry\_before\_Tnnn, before\_Tnnn, Tnnn or Tnnn\_dry, nnn being the test number

Type of data: ply mesh files

Units of data: m

Organization of files in directories: the 7z file is stored in the folder\subfolder sequence that depends on the context above

yyyy-nn-dd\Test\_nnn\before\_filling\region, if context is dry\_before\_Tnnn

yyyy-nn-dd\Test\_nnn\beginning\region, if context is before\_Tnnn

yyyy-nn-dd\Test\_nnn\end\region, if context is Tnnn

yyyy-nn-dd\Test\_nnn\tank\_empty\_end\region, if context is Tnnn\_dry

## **11.6 Remarks**

Measurements were made from 2017-11-01 to 2017-11-08.

## 12 Instrumentation – Thermal camera (UdCoruna)

### 12.1 Instruments

One Thermal camera with structured infrared light model BOBCAT-320 GigE;  
Aluminium rail 2,0 m above the wave tank bottom.

### 12.2 Measured parameters

Measure run-up and overtopping events during the test.

### 12.3 Experimental procedure

The camera was placed above the crest of the breakwater, after the entrance to the overtopping reservoir 3, but still in the breakwater trunk.

For the measurement with this camera, images with a frequency of 25 Hz have been captured. In addition, a heat emitting light was used to heat the Antifer cubes of the armour layer prior to the start of the tests. In this way, the water will have a darker color when it is colder than the blocks.

Finally, with the analysis of the camera, it is possible to obtain results of the overtopping.

### 12.4 Data post-processing

The result obtained has been processed with an in-house MATLAB algorithm. However, it was not possible to estimate the overtopping of the tests since the temperature of the blocks ended up being the same as that of the water, with no overflow results.

Finally, it has been possible to detect that it is a good methodology for the study of Run-up in breakwaters with few overtopping events.

The next figure shows an example of three images recorded with the thermal camera, the left one represents the initial situation, the middle one shows an example of the first overtopping event, and finally, the right one shows the final situation.



Provided datasets contain raw data without post-processing.

### 12.5 Organization of data files

Format: .7z

File name: Tnnn\_thermal\_UdCoruna.7z, nnn being test number. It contains the 284 x 288 pixel .png files with the frames, each identified with a serial number, taken during test nnn.

Organization of files in directories: each file is stored in the corresponding test\_nnnn\during directory

### 12.6 Remarks

Measurements were made from 2017-11-01 to 2017-11-08.

## **13 Instrumentation – 3D Laserscan (LUHannover)**

### **13.1 Instruments**

One 3D Laser Scanner (Faro Focus 3D) placed on a tripod, about 1.7 m above the basin floor.

Resolution in 10m distance: 0.4 mm

Repetition of each point measurement for accuracy: 8 times

Auto-Positioning and calibration by 10 ball-makers in the basin (each with 100 mm diameter)

### **13.2 Measured parameters**

Three-dimensional coordinates of point clouds resulting from 3D laser scan (m).

### **13.3 Experimental procedure**

The laser scanner is placed on the tripod at three positions around the breakwater head. Positions are chosen so that all marker balls are visible, and the breakwater slopes are unblocked visible.

### **13.4 Data post-processing**

Provided datasets contain raw data without post-processing.

### **13.5 Organization of data files**

Format: .7z

File name: context\_laserscan\_LUHannover.7z;

context explains how the data was obtained: dry\_before\_Tnnn or Tnnn\_dry, nnn being the test number

Type of data: .fls and .jog files

Units of data: n.a.

Organization of files in directories: the 7z file is stored in the folder\subfolder sequence that depends on the context above

yyyy-nn-dd\Test\_nnn\before\_filling\region, if context is dry\_before\_Tnnn

yyyy-nn-dd\Test\_nnn\tank\_empty\_end\region, if context is Tnnn\_dry

### **13.6 Remarks**

Scans were conducted before test 017, after test 020, before test 064 and after test 072.

## 14 References

Gronz, O., Hiller, P.H., Wirtz, S. and Ries, J.B. (2016) Smartstones: A small 9-axis sensor implanted in stones to track their movements, *Catena*, 142, 245-251.

Hofland, B., Arefin, S.S., Van der Lem, C. & Van Gent, M.R.A. (2018): Smart Rocking Armour Units. In: *Proceedings of the 7th International Conference on the Application of Physical Modelling in Coastal and Port Engineering and Science (Coastlab18)*, Santander.

Maciñeira, E., Burcharth, H.F. (2016). Stability of cube armoured roundheads exposed to long crested and short crested waves. *Coast. Eng.*, 112, 99-112.

Pedro, F., Bastos, M., Lemos, R., Fortes, C. and Santos, J.A. (2015) Toe berm damage progression analysis using a stereophotogrammetric survey technique, *Proc. 7th SCACR - Int. Short Course/Conf. on Applied Coastal Research*, Florence.

Van Gent, M.R.A. (2014) Oblique wave attack on rubble mound breakwaters, *Coast. Eng.* 88, 43-54.